Supplementary Material (ESI) for Chemical Communications

Synthesis and Structure of a Platinum(II) Molecular Square Incorporating Four Fluxional Thiacrown Ligands: The Crystal Structure of $[Pt_4([9]aneS_3)_4(4,4'\text{-bipy})_4](OTf)_8$

Daron E. Janzen, Ketankumar N. Patel, Donald G. VanDerveer and Gregory J. Grant*

Experimental

1. Materials

The reagents, [9]aneS_3 (1,4,7-trithiacyclononane), 4,4'-bipy (4,4'-bipyridine), silver triflate and silver hexafluorophosphate were purchased from Aldrich Chemical Company and used as received. All solvents were used as received. The Pt(II) complex, [Pt([9]aneS_3)Cl_2] was prepared by the literature method [S1].

2. Measurements

Analyses were performed by Atlantic Microlab, Atlanta, GA. All ^{1}H, $^{195}Pt\{H\}$ and $^{13}C\{H\}$ NMR spectra were obtained at 298 K on a Varian Gemini 300 MHz NMR spectrometer. The solvent CD_3NO_2 was employed for both the deuterium lock and reference for proton and carbon spectra. Platinum-195 NMR spectra were recorded at 25 °C and 64.270 MHz using aqueous solutions of $[PtCl_6]^{2-}$ (0 ppm) as an external reference with a delay time of 0.01 seconds. Referencing was verified versus authentic samples of $[PtCl_4]^{2-}$ which was found to have a chemical shift at -1626 ppm, in agreement with the reported value of -1624 ppm. [S2]. UV-vis spectra were obtained in acetonitrile using a Varian Cary Bio 100 UV-vis spectrophotometer. Infrared spectra were obtained on a Nicolet FT-IR using dry pre-weighed KBr packets (500 mg) equipped with an ATR accessory. Mass spectra were obtained on a BioTOF II ESI Mass spectrometer using a scan range of 100-1000 amu.

3. Preparation of $[Pt_4([9]aneS_3)_4(4,4'\text{-bipy})_4](SO_3CF_3)_8$: Molecular Square

A mixture of $Pt([9]aneS_3)Cl_2$ (100 mg, 0.224 mmol) and $AgSO_3CF_3$ (115 mg, 0.448 mmol) was stirred in 10 mL of CH_3CN for 24 hrs. The white precipitate (AgCl) was removed by filtration, and a mass of 4,4'-bipyridine (4,4'-bipy, 35.0 mg, 0.224 mmol) was added to the solution which was then stirred for 6 days. The solution was concentrated on a rotary evaporator to 1/3 of its original volume. Ether was slowly added to the solution to form yellow crystals of $[Pt_4([9]aneS_3)_4(4,4'\text{-bipy})_4](SO_3CF_3)_8$ (80.0 mg, 43.0%). A crystal suitable for X-ray diffraction was obtained by diffusing ether into a nitromethane solution. Analysis calculated for $C_{74}H_{94}F_{24}N_{10}O_{32}Pt_4S_{20}$. C, 25.29; H, 2.70; N, 3.99; S, 18.25. Found: C, 25.36; H, 2.72; N, 3.97; S, 18.06. FT-IR (KBr, cm^{-1}): 3094.6, 3025.6, 2986.8, 1615.8, 1533.9, 1417.5, 1253.7, 1167.4, 1029.5, 818.2, 753.5, 641.4, 572.7, 520.7. ^{1}H-NMR (ppm, CD_3NO_2), δ: 9.14 (pseudo-doublet (6.9 Hz) 16 H, 4,4'-bipy), 7.96 (pseudo-doublet (7.0 Hz), 16 H, 4,4'-bipy), 3.25 (b m, AA'BB' pattern, 48 H, ([9]aneS$_3$). ^{13}C{^{1}H}-NMR (ppm, CD_3NO_2), δ: 157.8 (16 C, 4,4'-bipy), 151.5 (16 C, 4,4'-bipy), 130.6 (8 C, 4,4'-bipy), 38.5 (24 C, [9]aneS$_3$). ^{195}Pt{^{1}H}-NMR (ppm, CD_3NO_2): -3134 ($\nu_{1/2}$ = 296 Hz) [3]. UV-vis (CH_3CN, λ_{max} nm (ε)): 273 (125,000). An ESI- Mass Spectrum of the complex shows one peak centered at 681 amu with the correct isotopic distribution patterns for $[Pt([9]aneS_3)(4,4'\text{-bipy})(OTf)]^{+1}$ (Molar mass = 680.90 amu). No higher mass peaks were observed.

4. Synthetic Scheme for Preparation of Molecular Square from [Pt([9]aneS$_3$)Cl$_2$]

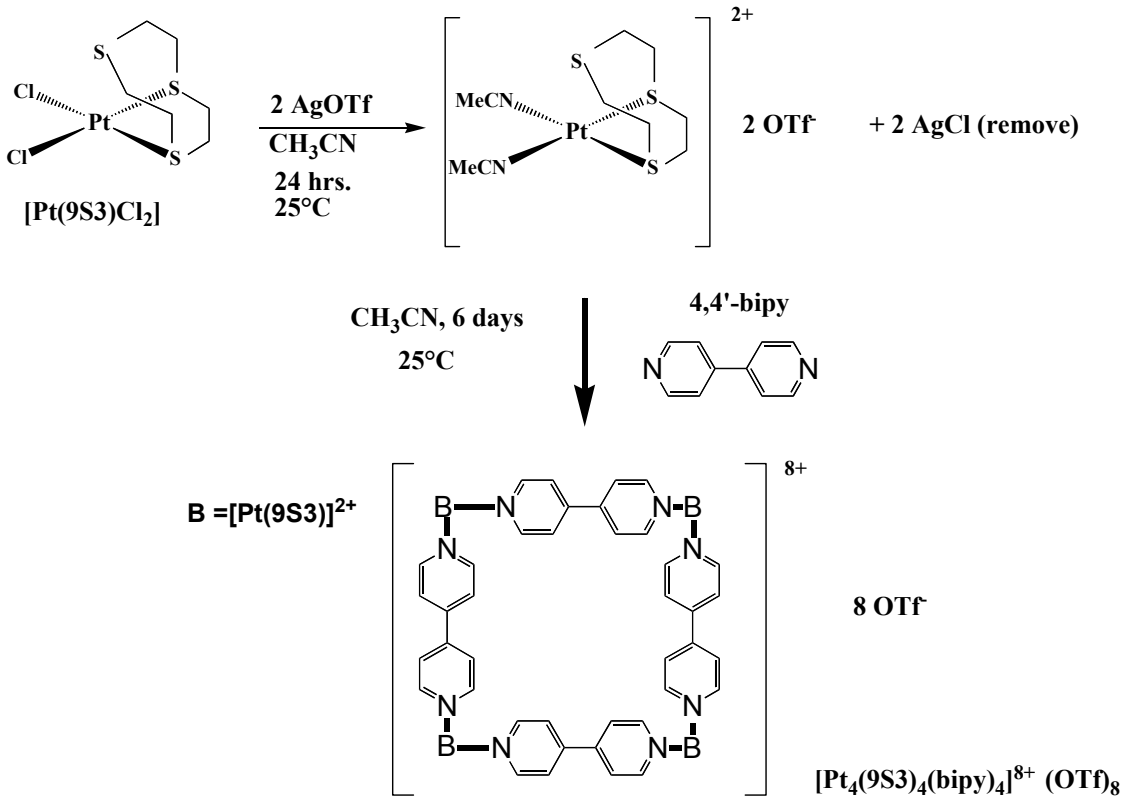

5. General Structural Features for $[Pt_4([9]aneS_3)_4(4,4'\text{-bipy})_4](SO_3CF_3)_8$

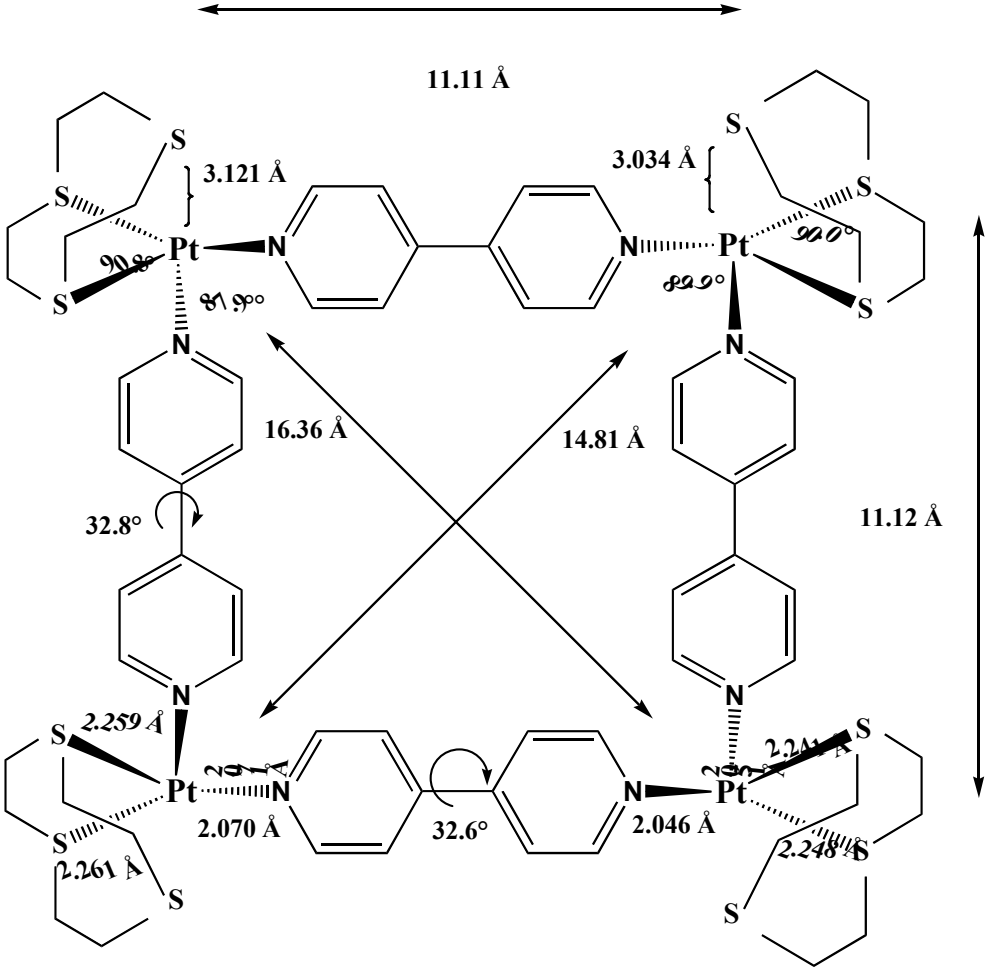

6. Multinuclear NMR spectra of $[Pt_4([9]aneS_3)_4(4,4'\text{-bipy})_4](SO_3CF_3)_8$

6.1 Proton NMR spectrum

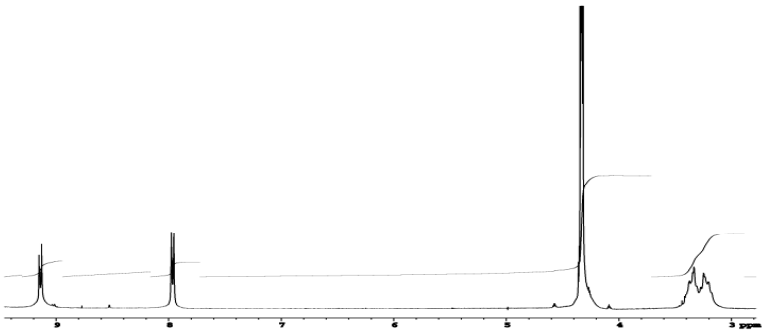

6.2 Carbon-13 NMR spectrum

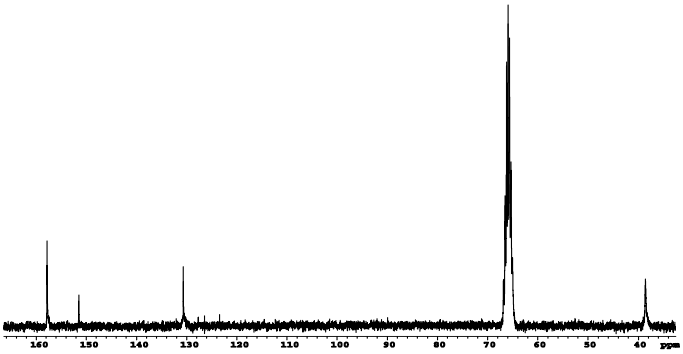

6.3 Platinum-195 NMR spectrum

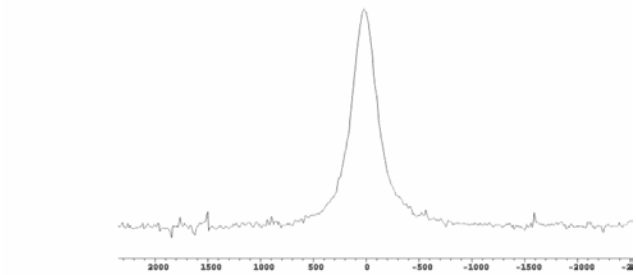

7. X-ray Structure Details for $[Pt([9]aneS_3)(bipy)]_4(OTf)_8$

Data collection

A crystal (approximate dimensions 0.19 x 0.12 x 0.12 mm^3) was placed onto the tip of a 0.1 mm diameter glass capillary and mounted on a CCD diffractometer for a data collection at 183(2) K. The data collection was carried out using MoKα radiation (graphite monochromator). The intensity data were corrected for absorption and decay (SADABS) [S4]. Final cell constants were calculated from the xyz centroids of 8769 strong reflections from the actual data collection after integration (SAINT) [S5]. Please refer to Table 1 for additional crystal and refinement information.

Structure solution and refinement

The structure was solved using SHELXS-97 [S6] and refined using SHELXL-97 [S6]. The space group C 2/c was determined based on systematic absences and intensity statistics. A direct-methods solution was calculated which provided most non-hydrogen atoms from the E-map. Full-matrix least squares / difference Fourier cycles were performed which located the remaining non-hydrogen atoms. All non-hydrogen atoms were refined with anisotropic displacement parameters. All hydrogen atoms were placed in ideal positions and refined as riding atoms with relative isotropic displacement parameters. The cationic structure component and charge balancing anions were located from the electron density map, and their positions and thermal parameters refined well. A nitromethane solvent molecule was apparent in the asymmetric unit in the e-map. Attempts to refine the nitromethane however were unsuccessful as it was highly disordered. The structure model at this point was R1 = 0.0947. The program PLATON/SQUEEZE was then used to remove electron density due to apparent and possibly unapparent solvent molecules and calculate approximate solvent accessible void space in the unit cell. The final full matrix least squares refinement after applying the SQUEEZE program converged to $R1 = 0.0780$ and $wR2 = 0.2099$ (F^2, all data).

Structure description

The structure consists of an 8^+ molecular square with 4,4'-bipyridine bridges between corners composed of Pt([9]aneS_3) units with 8 charge balancing triflate anions. Each square is composed of 4 Pt([9]aneS_3) corners and four 4,4'-bipy linkers as sides to the square. The asymmetric unit however consists of only 2 corners linked by one bipy ligand, and two halves of a bipy ligand (one half each bonded to each unique Pt center (figure 2). The square is completed by the C_2 axis at the center of a square which relates

the asymmetric unit to the other half of a given square. Each unique Pt center shows two sulfurs of a [9]aneS_3 ligand coordinated to the metal and the third sulfur with an axial interaction closer than van der Waals contact (Pt1-S1 distance = 3.0344 Å (35), Pt2-S4 distance = 3.1214 Å (30)). One [9]aneS_3 ligand of the asymmetric unit displayed disorder which was modeled. The disorder components are two slightly different ligand conformations of [9]aneS_3 which refined to a ratio of occupancy 48/52 (minor component atom names C3, C4, C5, C6; major component atom names C3', C4', C5', C6'). As a part of the disorder model, atoms C3 and C6 were constrained to have identical positions to C3' and C6', respectively. Thermal parameters of pairwise disorder component atoms were also constrained to be equal (C3 and C3', C4 and C4', C5 and C5', C6 and C6'). The Pt-N distances are similar for each unique Pt (Pt1-N1 2.070(8) Å , Pt(1)-N2 2.071(9) Å, Pt2-N3 2.046(9) Å, Pt2-N4 2.051(9) Å). Note the slightly longer Pt-N distances of Pt1 correlate with the shorter Pt-S axial distances. The Pt-S bond distances are also similar for each unique Pt (Pt1-S2 2.259(3) Å, Pt1-S3 2.261(3) Å, Pt2-S5 2.241(3) Å, Pt2-S6 2.248(3) Å). Again, note how the longer Pt-S bond distances of Pt1 correlate with the longer Pt-N distances and shorter Pt-axial sulfur distance. Of interest is also the twist in the 4,4'-bipy ligands, where the angle between least-squares planes of the pyridine rings is significantly twisted (32.6° for N1, C13-C17 to N4, C28-C32, 34.9° for N2, C18-C22 to N3, C23-C27).

Though evidence for a nitromethane molecule per asymmetric unit was present in the electron density map, efforts to model the disorder in the solvent molecule were unsuccessful. A program to remove residual disordered solvent was applied to the structure solution without nitromethane. The results of this treatment (SQUEEZE, [S7]) yielded better refinement statistics but unexplained residual electron density is still present in the structure (maximum residual positive electron density 7.518 e-/Å^3, minimum residual negative electron density -2.141 e-/Å^3). The SQUEEZE program located 4 solvent accessible voids in the structure. The summary of the description of the voids is as follows:

Void #	xfrac	yfrac	zfrac	V(Å^3)	Number of e-
1	0.250	0.750	0.000	501.2	44.1
2	0.750	0.250	0.000	501.2	44.1
3	0.250	0.250	0.500	501.3	41.1
4	0.750	0.750	0.500	501.3	41.1

The sizes of the voids are large enough to hold the solvent molecules indicated form a bulk sample elemental analysis. The elemental analysis indicates 2 nitromethane and 4 water solvate molecules per $[Pt([9]aneS_3)(bipy)]_4[OTf]_8$ unit. These solvate molecules would require 237 $Å^3$ (72.5 $Å^3$/nitromethane, 23 $Å^3$/water estimated from atomic volumes [S8] per formula unit (Z = 4 so each hole is needed to accommodate 2 nitromethanes and 4 waters). In other words, each hole is large enough to accommodate solvate molecules indicated by the elemental analysis. Disordered solvent also takes up more volume than ordered solvent so extra volume is reasonable. As residual electron density remains in non-void regions of the structure, the number of electrons indicated by the SQUEEZE procedure in each void is likely inaccurate. The location of the voids is also interesting. The figures and discussion regarding this structure indicate that triflates occupy the space inside each square. The coordinates of the voids accordingly do not correspond to the center of the squares in the unit cell.

Many parameters of this structure are better understood in the context of the only other Pt-bipy bridged square structures crystallographically characterized to date [S9]. One such structure is a Pt bipy bridged structure with bis(diphenylphosphino)propane on each Pt corner published by Stang [S10]. The anions in this structure are also triflates and are only partially located in the structure. The other such structure is that published by Fujita which has ethylenediamine ligands on the Pt corners, 14 nitrates, 12 waters, and 3 trans-$Pt^{IV}Br_2(en)_2$ 2+ cations in the formula unit [S11]. The trans-$Pt^{IV}Br_2(en)_2^{2+}$ cations fill the square holes. Comparison of these two structures with the structure of $[Pt([9]aneS_3)(bipy)]_4(OTf)_8$ are made using the .cif files obtained from the Cambridge Structural Database and with the program Mercury [S12].

The twist of the square away from a planar structure is evident through several different parameters. Significant twist in the square is not rationalized through the N-Pt-N angles (N1-Pt1-N2 89.9(4)°, N3-Pt2-N4 87.9(4)°). By comparison of the Pt-Pt distances (11.11 Å and 11.12 Å) in this square relative to the two other bipy bridged Pt squares (Stang 11.09 Å, Fujita 11.12 Å) slight differences are observed. A better measure of the puckering of a square can be quantified by calculating the displacement from a least-squares plane calculated using the 4 corner positions of a square. In this structure, each Pt is displaced 0.68 Å from the lsq plane. In the other structures, larger puckering is observed in Stang's square (Pt atoms displaced 1.87 Å) and no puckering in Fujita's

square (Pt atoms displaced 0.0 Å).

The occupancy of the holes in the current structure is interesting in that 4 triflate anions fill each square hole. Many close F-F interactions dominate the triflate placement in the square holes. All the anionic SO_3 groups of the triflates point away from the holes, while the CF_3 groups all point in toward the square holes. Two of the triflates have unique positions and the inversion center at the center of the square generates the additional two trilfates to fill the hole. The two unique triflates in the square holes are identified as F1-F3, C36, S10, O10-O12 and F4-F6, C35, S9, O7-O9. There are 9 F-F intermolecular F-F distances between triflates less than VDW sum + 0.5 Å (1.47 Å *2 + 0.5 = 3.44 Å) inside each square (5 of which are unique). The other 4 triflates (per formula unit) gather in regions between squares in a similar fashion. The two unique triflates as identified as F10-F12, C33, S7, O1-O3 and F7-F9, C34, S8, O4-O6. The other two triflates that lie outside of the hole cluster are generated by an inversion center. There are 9 F-F intermolecular F-F distances between triflates less than VDW sum + 0.5 Å (1.47 Å *2 + 0.5 = 3.44 Å) outside each square (5 of which are unique). In the Stang square, it is unclear whether solvent or anions are in pocket. In Fujita's square, each square contains a trans-$Pt^{IV}(en)_2Br_2^{2+}$ inside the square hole.

In terms of channels formed by the holes in the squares, this structure has all squares aligned to form channels that are parallel with the b axis of the unit cell. Stang's square has a similar channel structure with channels aligned along the b-axis. In Fujita's square, the square holes do not form channels but channels exist in between squares that are filled with nitrate anions and trans-$Pt^{IV}(en)_2Br_2^{2+}$ cations. The orientation of the squares to one another determines whether channels are found in the structure or not. In the case of our square, each square is exactly one length of the b-axis apart from the next square in the channel, 13.987 Å. Stang's structure is similar but the b-axis is longer, 15.689 Å, as the bis(diphenylphosphino)propane ligands are more sterically demanding intermolecularly than [9]aneS_3. In Fujita's square, each square is oriented at 90° to other squares in a totally different packing arrangement. In part this might be due to the sterically undemanding ethylenediamine ligands at the Pt corners.

Packing of the squares can be described as alternating layers of squares that are displaced half the length of the unit cell parameters a and c from one another. The layers packing motif is ABAB. One type of channel in the structure extends along the b axis through the squares in all layers of A. Similarly, a second type of channel in the structure extends

along the b axis through the squares in all layers of B. A third unique type of channel extends through the space between square holes through all layers. As previously discussed the channels formed by the square holes are filled with triflates. The channels in between square hole channels are also filled with triflates.

Data collection and structure solution were conducted at the X-Ray Crystallographic Laboratory, Clemson University.

Table 1. Crystal data and structure refinement for grant62d.

Identification code	grant62d	
CCDC	609042	
Empirical formula	C72 H80 F24 N8 O24 Pt4 S20	
Formula weight	3319.00	
Temperature	183(2) K	
Wavelength	0.71073 Å	
Crystal system	Monoclinic	
Space group	C 2/c	
Unit cell dimensions	a = 33.022(7) Å	α = 90°
	b = 13.987(3) Å	β = 95.24(3)°
	c = 26.107(5) Å	γ = 90°
Volume	12008(4) Å^3	
Z	4	
Density (calculated)	1.836 Mg/m^3	
Absorption coefficient	5.093 mm^{-1}	
F(000)	6432	
Crystal color, morphology	orange, block	
Crystal size	0.19 x 0.12 x 0.12 mm^3	
Theta range for data collection	2.79 to 25.10°	
Index ranges	$-39 \le h \le 39$, $-16 \le k \le 16$, $-31 \le l \le 31$	
Reflections collected	40509	
Independent reflections	10663 [R(int) = 0.0852]	
Observed reflections	8769	
Completeness to theta = 25.10°	99.7%	
Absorption correction	Semi-empirical from equivalents	
Max. and min. transmission	0.5453 and 0.4178	
Refinement method	Full-matrix least-squares on F^2	
Data / restraints / parameters	10663 / 0 / 692	
Goodness-of-fit on F^2	1.076	
Final R indices [I>2sigma(I)]	R1 = 0.0780, wR2 = 0.2006	
R indices (all data)	R1 = 0.0907, wR2 = 0.2099	
Largest diff. peak and hole	7.518 and -2.141 e.Å^{-3}	

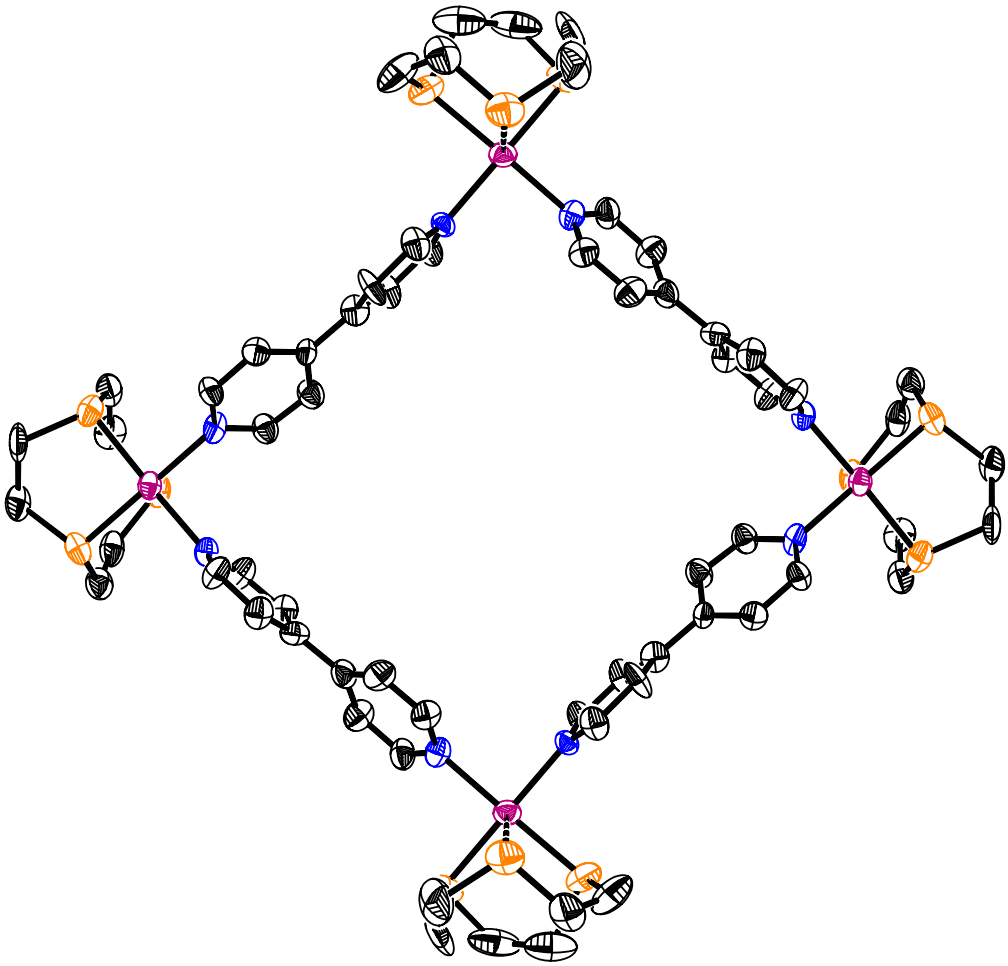

ORTEP of square 8+ cation (50% probability ellipsoids, triflates and [9]aneS_3 disorder omitted for clarity).

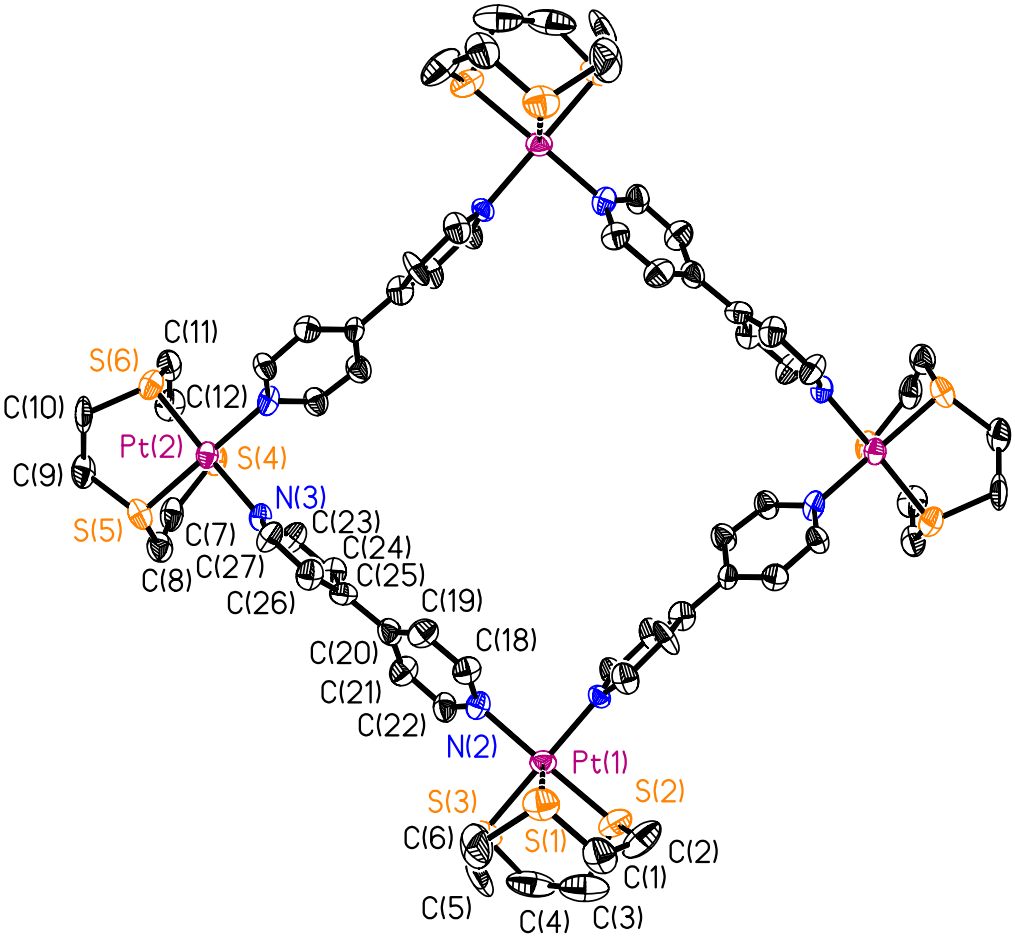

ORTEP of square 8+ cation with labels (50% probability ellipsoids, triflates and [9]aneS_3 disorder omitted for clarity).

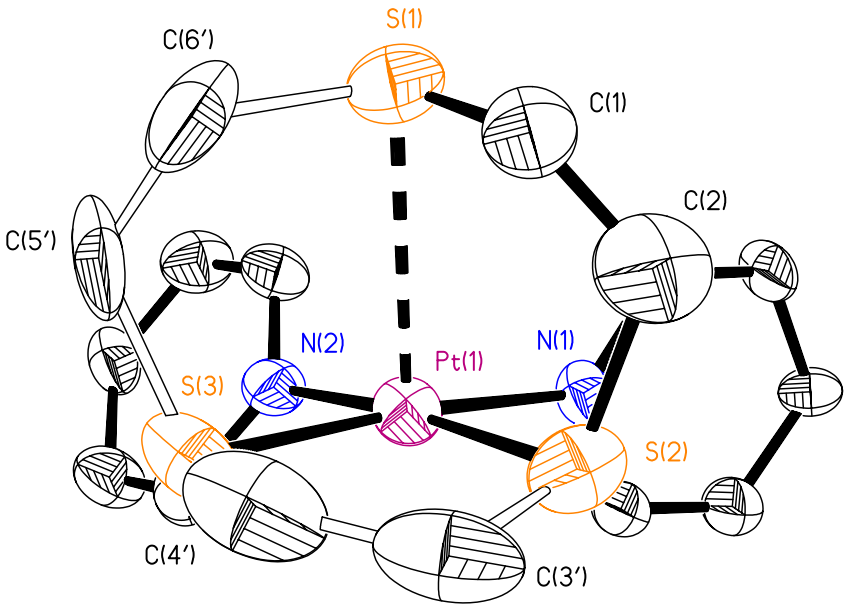

Figure showing minor disorder component of one [9]aneS$_3$ ligand (50% ellipsoids).

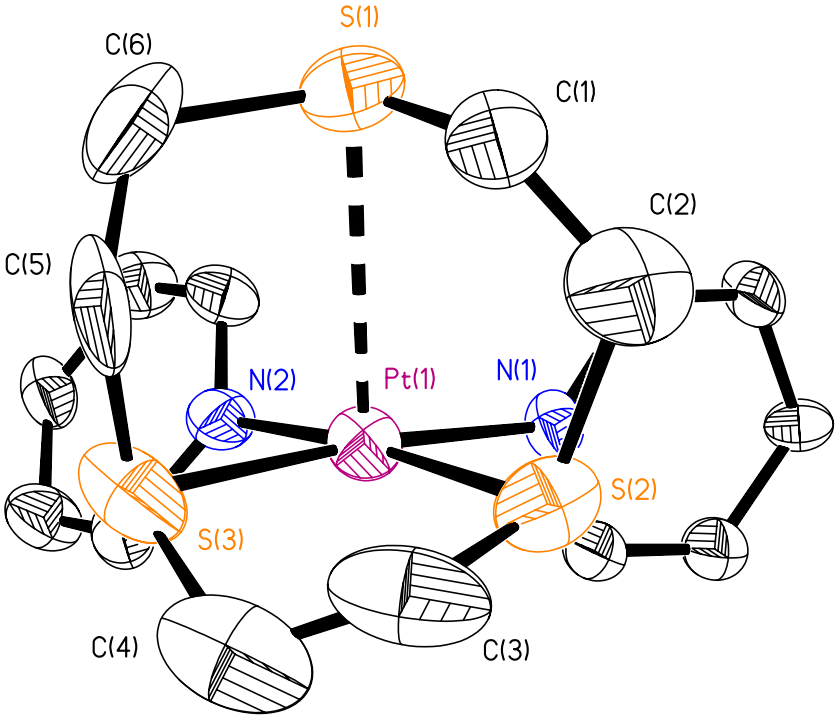

Figure showing minor disorder component of one [9]aneS$_3$ ligand (50% ellipsoids).

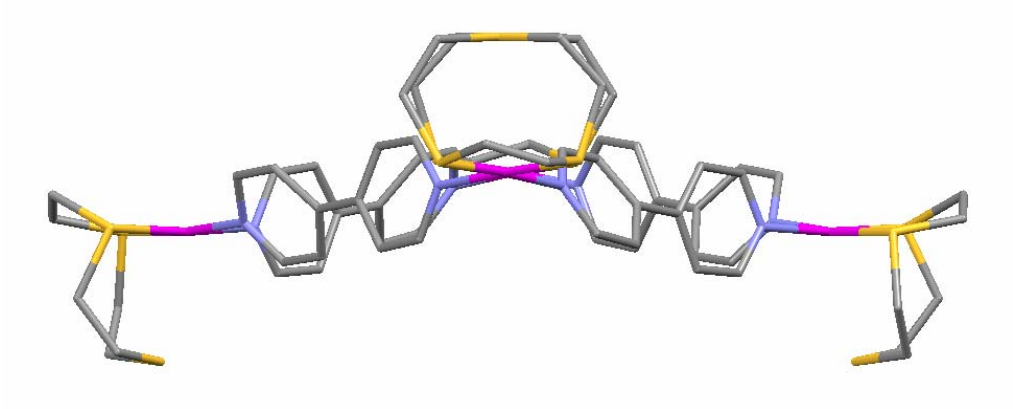

Figure showing the twist in the square 8+ cation.

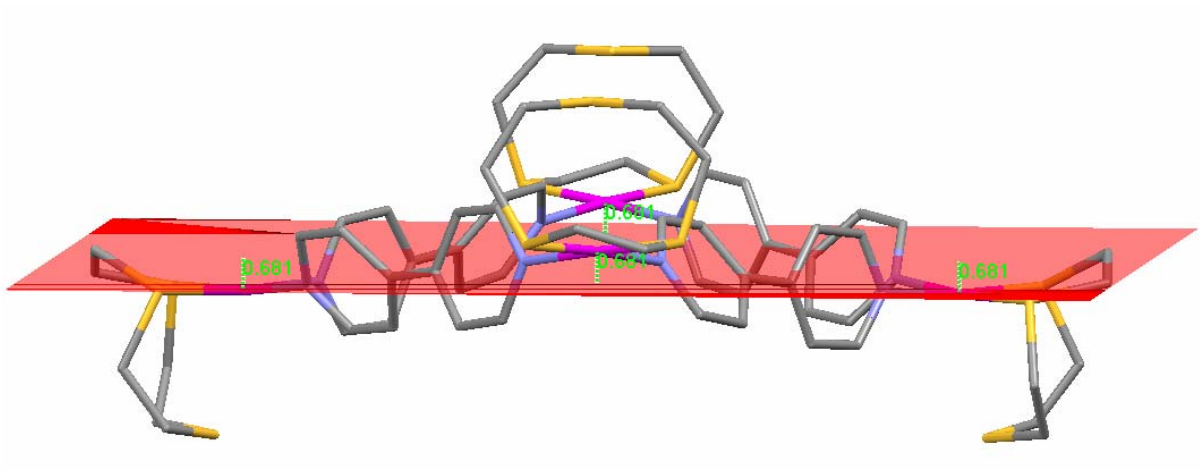

Figure showing displacement from a least-squares plane formed by the Pt atoms.

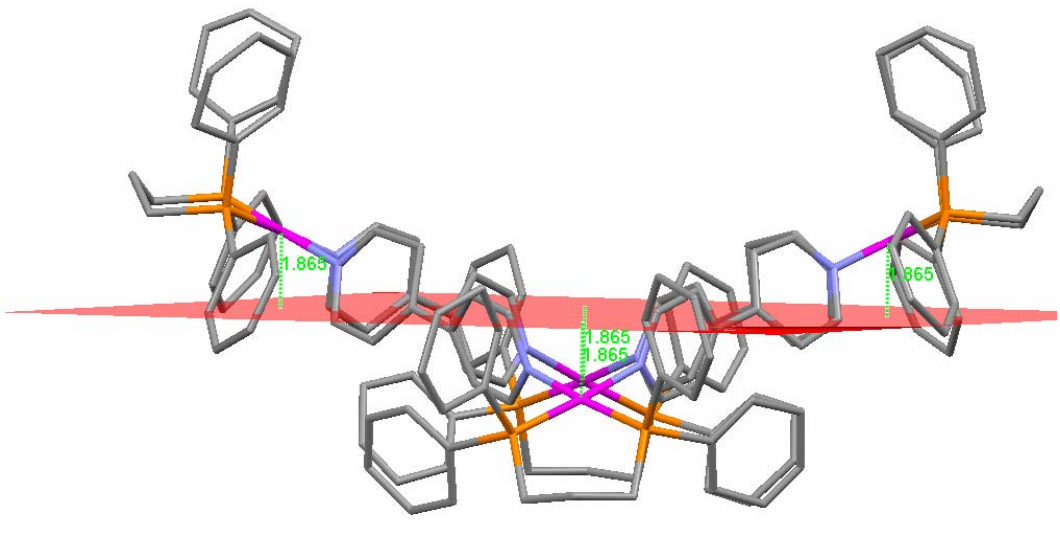

Stang's square twist figure with displacement from a least-squares plane formed by the Pt atoms. There is significant twist from a square plane.

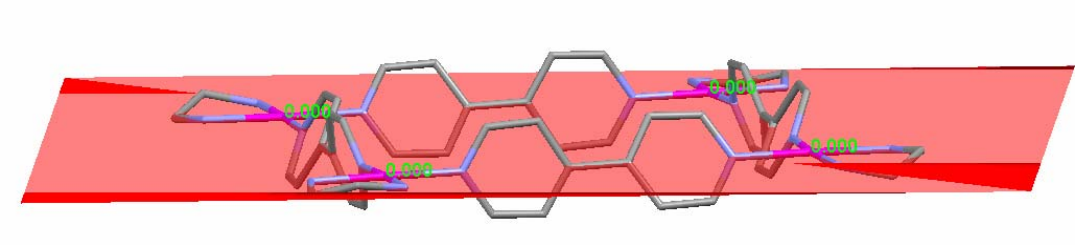

Fujita's square twist figure with displacement from a least-squares plane formed by the Pt atoms. The Pt atoms form a perfect plane, with no displacement from a least-squares plane formed by the 4 Pt corners.

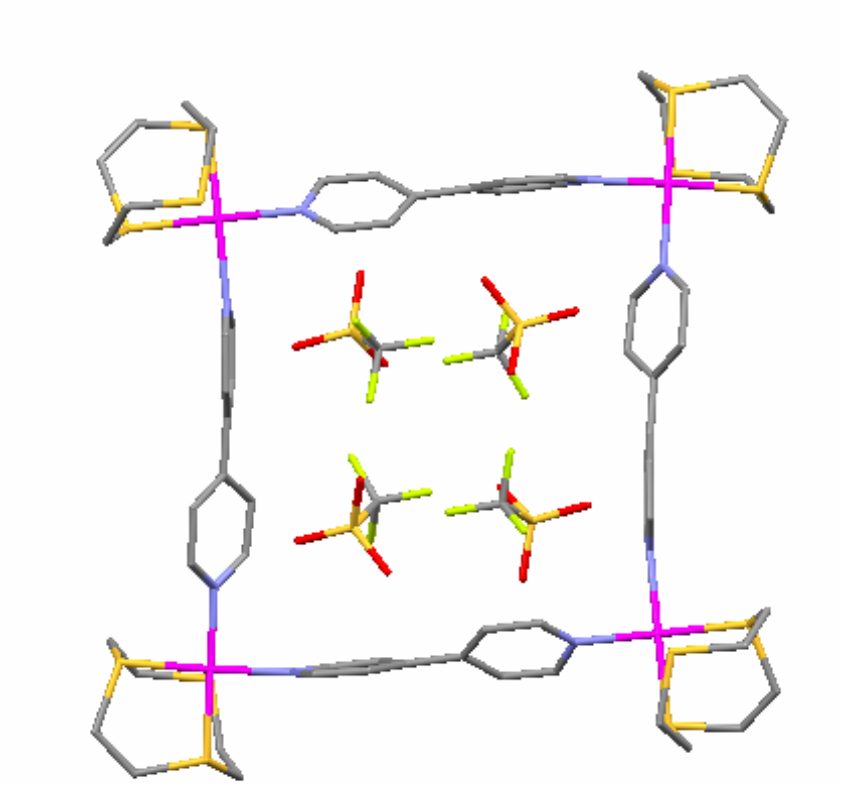

Line drawing showing triflates inside the square cavity.

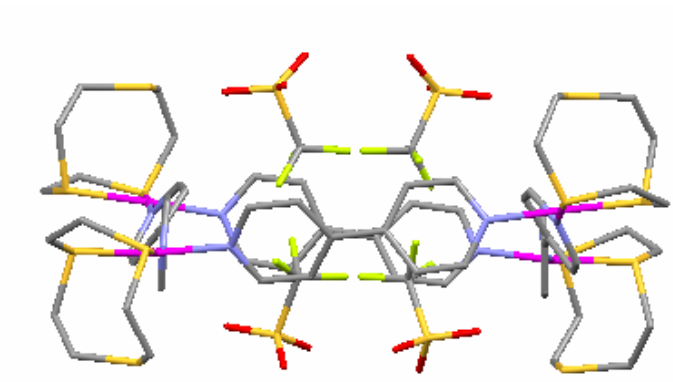

Line drawing showing triflates inside the square cavity, viewed 90° to previous figure, showing that the triflates are inside the square cavity.

Space-filling model showing triflates inside the square cavity.

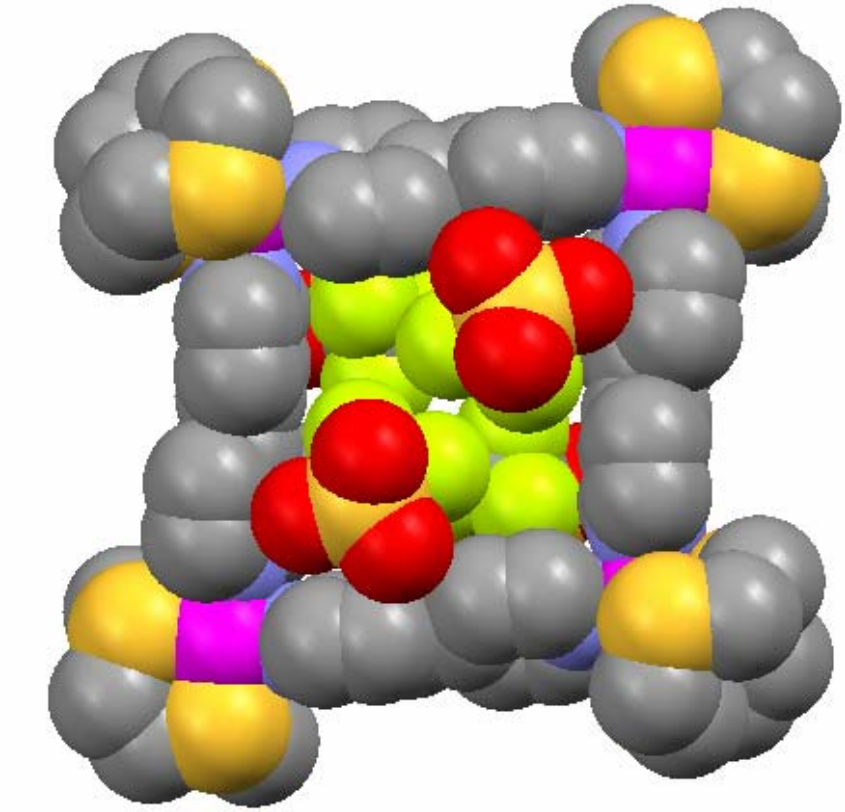

Space-filling model showing triflates inside the square cavity, viewed 90° to previous figure, showing that the triflates are inside the square cavity.

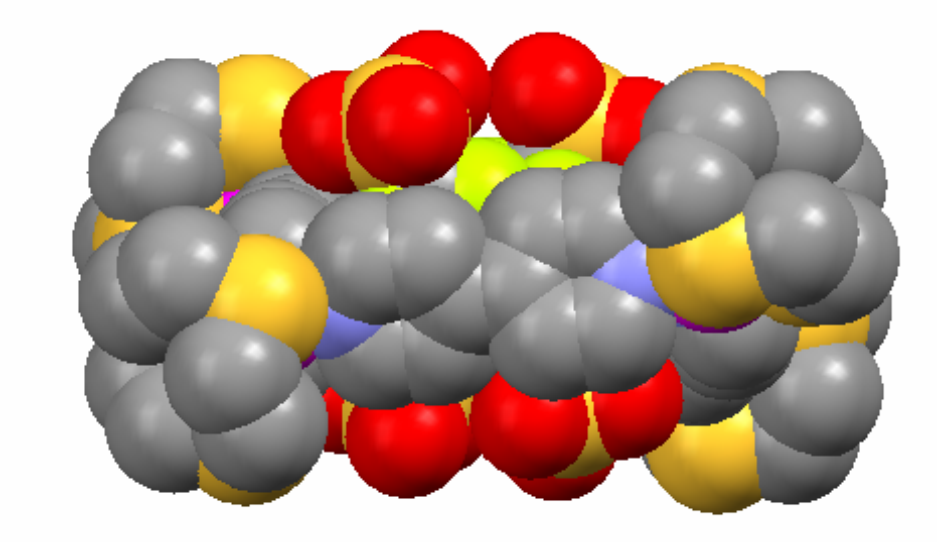

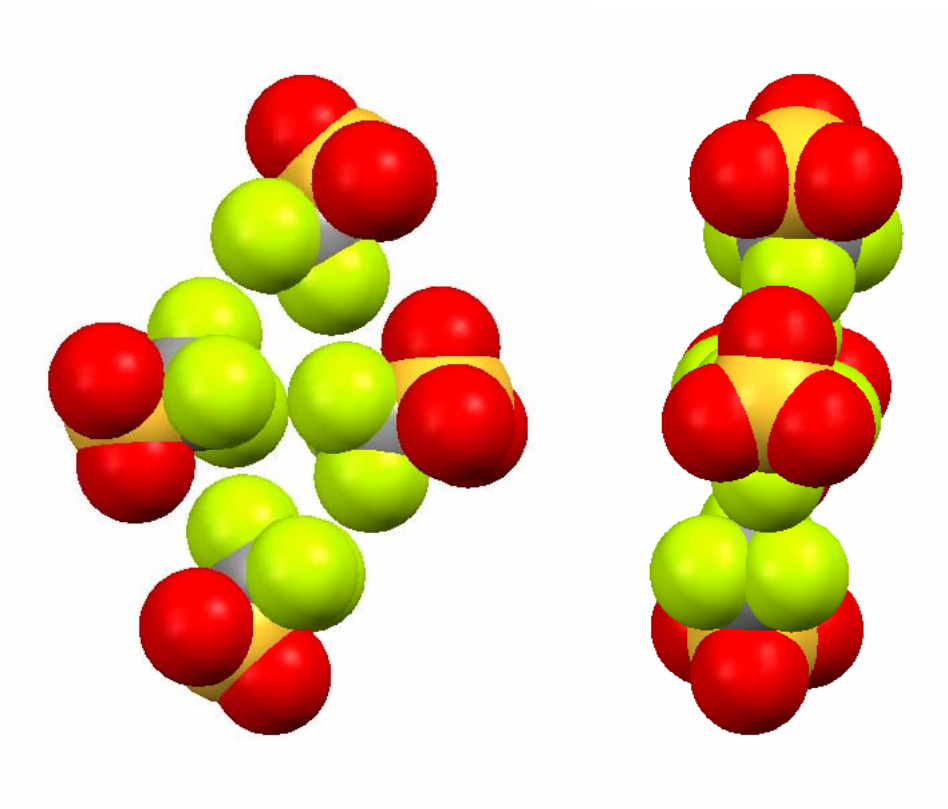

Space-filling model showing the cluster of triflates located outside the squares(left), another view at 90° (right).

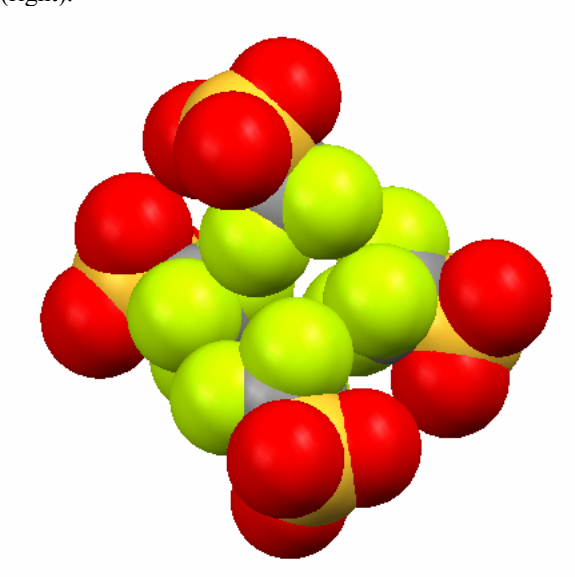

Space-filling model showing the cluster of triflates located inside the square cavity (left), another view at 90° (right). This cluster of triflates is more tightly associated in a more spherical nature, compared to a somewhat planar, more loosely associated outside triflate cluster.

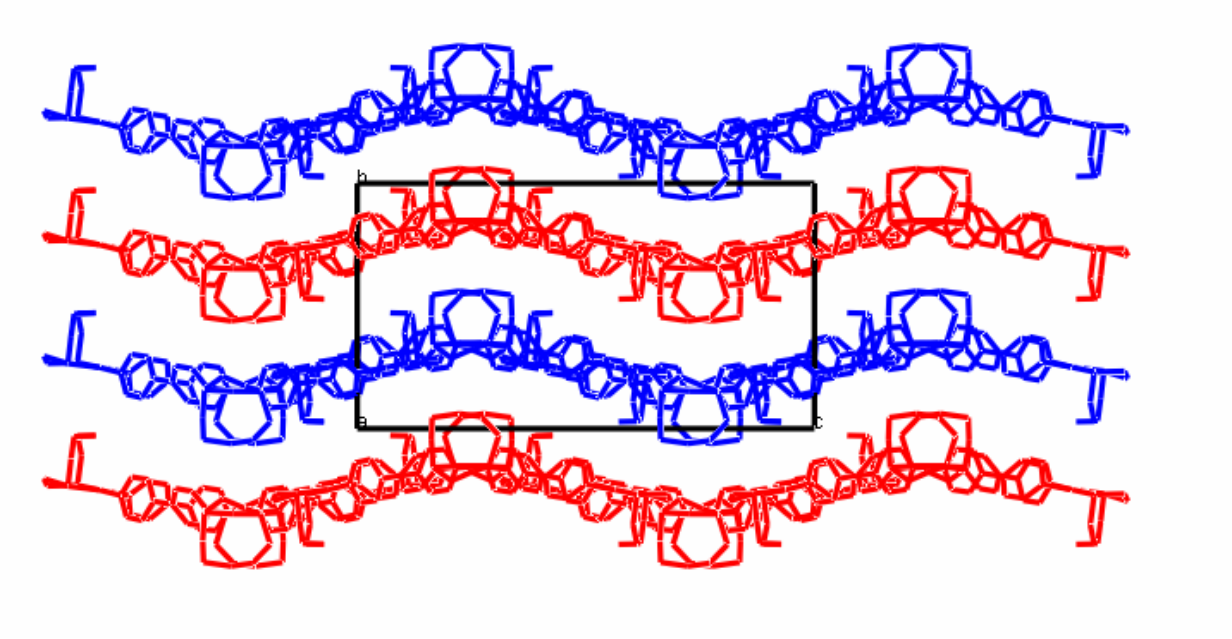

Packing diagram viewed parallel to the a-axis. Red squares are all in a given layer. Blue squares are all in a different layer. This shows the ABAB stacking motif.

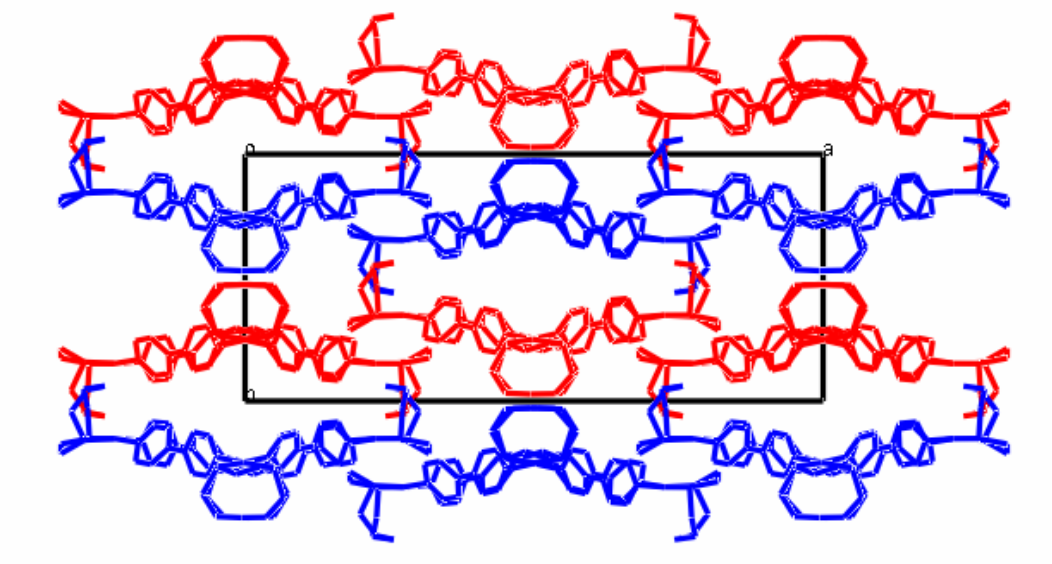

Packing diagram viewed parallel to the c-axis. Red squares are all in a given layer. Blue squares are all in a different layer. This shows the ABAB stacking motif.

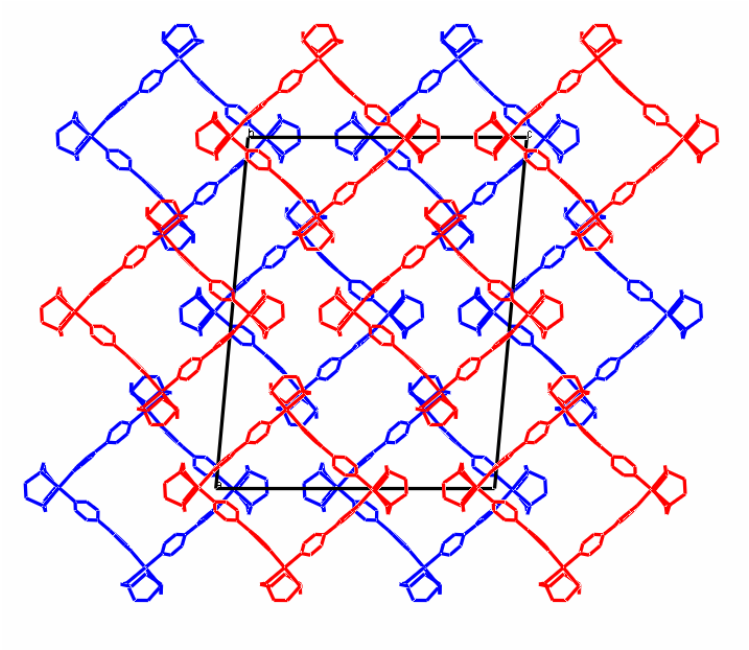

.

Packing diagram viewed parallel to b-axis. Red squares are all in a given layer. Blue squares are all in a different layer.

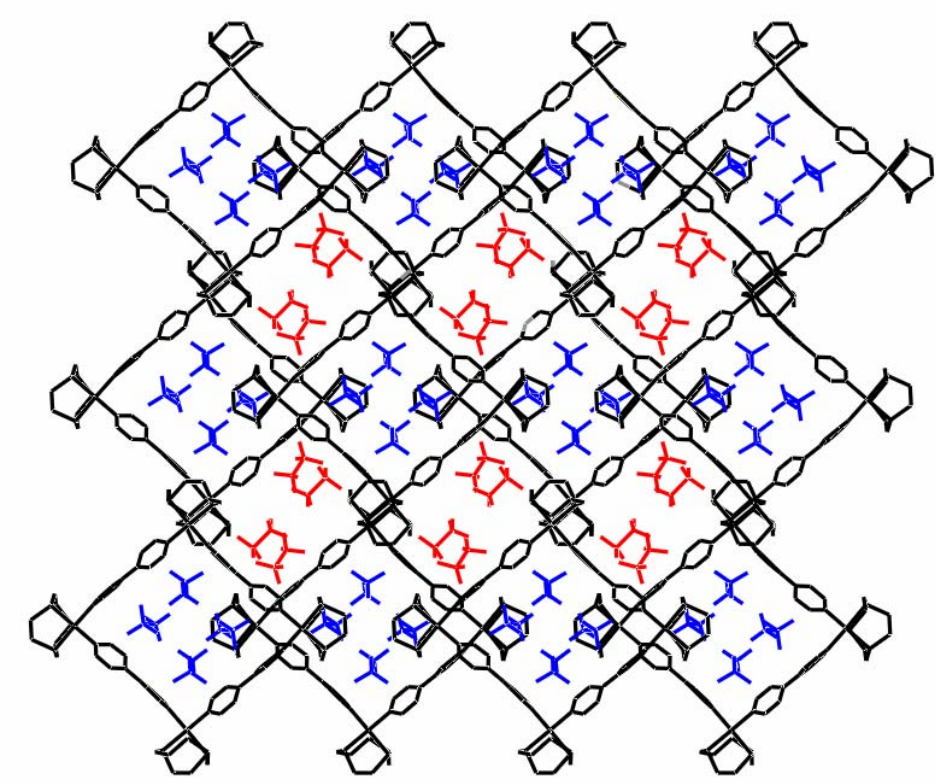

Packing view looking parallel to the b axis. Red triflates are in between squares. Blue triflates are inside the square cavities.

References

[S1] G.J. Grant, *Inorganic Synthesis,* 2006**,** submitteds.

[S2] P.S. Pregosin, in *Transition Metal Nuclear Magnetic Resonance*, ed. P.S. Pregosin, Elsevier, New York, 1991; page 251, and references cited therein.

[S3] *Bis* monodentate pyridine ligands typically show downfield ^{195}Pt NMR shifts compared to the analogous bidentate bipyridyl ligands. As a specific example, [Pt(2,2'-bipy)Cl_2] shows a chemical shift of -2315 ppm while *cis*-[Pt(py)$_2$$Cl_2$] has a downfield value of -1998 ppm. See E.G. Hope, W. Levason, N.A. Powell, *Inorg. Chim. Acta,* 1986, **115***,* 187; C. Tessier, F.D. Rochon, *Inorg. Chim. Acta,* 1999, **295,** 25. The chemical shift we observe here is consistent with the trend since the molecular square shows a 130 ppm downfield chemical shift compared to the ^{195}Pt NMR resonance at -3261 ppm for [Pt([9]aneS_3)((bipy)]^2. G.J. Grant, K.N. Patel, M.L. Helm, L.F. Mehne, D.W. Klinger, D.G. VanDerveer, *Polyhedron*, 2004, **23,** 1361.

[S4] An empirical correction for absorption anisotropy, R. Blessing, *Acta Cryst.* 1995, **A51**, 33.

[S5] SAINT V6.2, Bruker Analytical X-Ray Systems, Madison, WI (2001).

[S6] SHELXTL V6.10, Bruker Analytical X-Ray Systems, Madison, WI (2000).

[S7] (a) P. Van der Sluis, A.L. Spek, *Acta Cryst.,* 1990, **A46***,* 194.; subroutine of PLATON A.L. Spek, *Acta Cryst.,* 1990, **A46***,* C34.
(b) PLATON – A Multipurpose Crystallographic Tool; Utrecht University, Utrecht, The Netherlands; A.L. Spek (2005)

[S8] *Acta Cryst.,* 1977, **A33***,* 216.

[S9] Recent search of the CSD v. 5.27 (through May 2006 update) reveals only two molecular square structures with 4,4'-bipy as linkers and Pt^{2+} corners (CSD structure codes LIQQUX and ZAGCIT)

[S10] P.J. Stang, D.H. Cao, S. Saito, A.M. Arif, *J. Am. Chem. Soc.,* 1995, **117***,* 6273.

[S11] M. Aoyagi, K. Biradha, M. Fujita, *Bull. Chem. Soc. Japan,* 1999, **72***,* 2603.

[S12] Mercury v 1.4.1. Cambridge Crystallographic Data Centre, 12 Union Road, Cambridge CB2 1EZ. U.K.